Research Report

2006-11

Permanent Magnet Machine Design Practice and Optimization

W. Ouyang, D. Zarko*, T.A. Lipo

Department of Electrical and Computer Engineering
University of Wisconsin-Madison
1415 Engineering Drive
Madison, WI 53706

*Department of Electrical Machines, Drives and Automation
University of Zagreb
Unska 3, HR-10000
Zagreb, CROATIA

Work performed at WEMPEC sponsored by CPES.

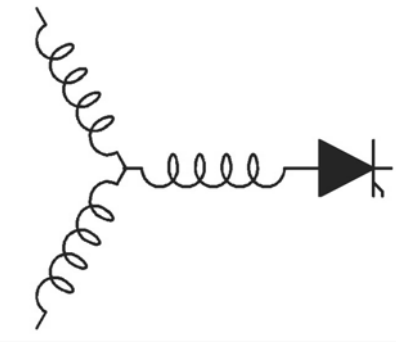

Wisconsin
Electric
Machines &
Power
Electronics
Consortium

University of Wisconsin-Madison
College of Engineering
Wisconsin Power Electronics Research Center
2559D Engineering Hall
1415 Engineering Drive
Madison WI 53706-1691

Permanent Magnet Machine Design Practice and Optimization

Wen Ouyang, Damir Zarko*, T.A.Lipo

Department of Electrical and Computer Engineering
University of Wisconsin-Madison
1415 Engineering Drive
Madison, WI 53706
Eamil: ouyang@cae.wisc.edu , lipo@engr.wisc.edu

*Department of Electrical Machines, Drives and Automation
University of Zagreb
Unska 3, HR-10000
Zagreb, CROATIA
Eamil: damir.zarko@fer.hr

***Abstract* — The complexity of the permanent magnet (PM) machine structure makes the optimal design of the PM machine always a difficult task. The multiple objectives of an optimal design make most classic optimization algorithms inapplicable, due to the nonlinearity and some discontinous variables. In this paper, two interior permanent magnet (IPM) machine design practices with modular stator structure and conventional stator structure are discussed. The design process is directly coupled with finite-element analysis (FEA) with the machine design guidelines embedded in the optimization process. Multivariable optimization methods based on Monte Carlo and Differential Evolution algorithms are applied in the design phase and the results are compared in this paper.**

***Keywords* — Permanent Magnet, Design Optimization, FEA, Differential Evolution (DE)**

I. INTRODUCTION

In a typical permanent magnetic machine design phase, an analytical machine model is usually developed first. If the machine model is sufficiently accurate, the optimization of the design can deliver dependable machine parameters and thus the machine performance can be accurately predicted. However, the nonlinearity of the materials generates errors in the analytical model compared with the FEA simulation, which is usually taken as the benchmark for analysis because of its dependable accuracy. Moreover, the increased complexity of the machine structure makes such an analytical procedure a tough task for each specific design, resulting in even more effort required for the correction of the analytical models, for instance, in the case of interior PM machine design, which is strongly coupled with rotor side iron saturation. Although the analytical machine model still plays an important role in the design phase by providing general relationship between main machine parameters and the details of machine performance [1][2][3], researchers still need to apply FEA simulations to validate their final design. Due to complexity of the design optimization with multiple variables, it is more practical to find an optimized design which satisfies the design objectives. In this paper, a general method for permanent magnet machine design coupled with the FEA analysis as a part of the optimization process is presented. Several permanent magnet design practices based on different optimization methods are discussed.

This work was supported in part by the ERC program of the National Science Foundation under award number EEC-9731677 for the Center for Power Electronic Systems.

II. MACHINE OPTIMIZATION

The specifications of a machine design are often in conflict, for instance, between high power density and low magnet volume. The machine parameters usually impact the machine final performance nonlinearly while they are highly coupled at the same time. Thus, it is difficult to distinguish the parameter choices that lead to a machine design which satisfies all the requirements. The machine design usually falls into a class of nonlinear, multiple-objective optimization problems with multiple constraints, as described by (1) to (4).

The design parameters:

$$\vec{x} = [x_1, x_2, \ldots, x_D], \ \vec{x} \in R^D \tag{1}$$

The design constraints:

$$g_j(\vec{x}) \le 0, \quad j = 1, \ldots, m \tag{2}$$

The boundary of the parameters:

$$x_i^{(L)} \le x_i \le x_i^{(U)}, \quad i = 1, \ldots, D \tag{3}$$

And the objective function set:

$$f(\vec{x}) = \left[f_1(\vec{x}), f_2(\vec{x}), \ldots, f_k(\vec{x}) \right] \tag{4}$$

Various optimization methods have been reported for use in the machine design. The heuristic methods play an important role among these methods. A specific mechanism of a stochastic method combined with a certain vector generation strategy is usually applied in the algorithm design to handle those uncertainties in the problem and seek good solution sets. An evolutionary algorithm and simulated annealing are typical modern heuristic methods that are based on some biological metaphor and thermodynamics respectively. In this paper, an evolutionary algorithm based method is applied in the machine optimization.

A typical evolutionary algorithm differs from the traditional

optimization algorithm in several aspects: encodes the control variables, rather than the variables themselves; operates on populations of solutions, rather than on individual solutions; uses objective function values, rather than derivatives. However, it must be noted that the classic evolutionary algorithm is found to have convergence difficulties and suffers from computational inefficiency. In this paper, the Differential Evolution (DE) algorithm introduced by Storn and Price in 1995 [4] has been selected for the machine design optimization. The algorithm structure is illustrated in Figure 1. The two main algorithm control parameters F and CR are defined as:

F: amplification constant, $0<F\leq 2$
CR: crossover probability, $0\leq CR\leq 1$

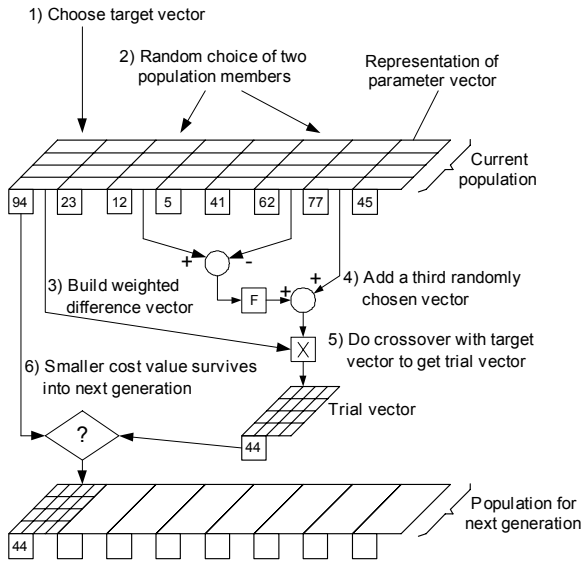

Figure 1: Differential evolution algorithm

Due to the complexity of the machine structure, it is not obvious how to locate the proper design parameters at the very beginning. The generation based selection of the optimization vectors does not require any special information when the initial vectors are generated. With the crossover and mutation mechanism embedded in the algorithm, the generation set is migrated gradually from the initially randomly generated set to the solution set which is confined by the optimization constraints. The result of the optimization is a population of solutions which belong to a Pareto optimal set. The vector of decision variables x_0 is Pareto optimal if there exists no other vector from the feasible space such that $f_i(x)<=f_i(x_0)$ for all $i=1,...,k$ and there exists at least one $i=1,...,k$ for which $f_i(x)<f_i(x_0)$.

For various applications it is necessary for the algorithm to take into consideration the special nature of each optimization goal, which benefits the optimization as well since the computation cost is reduced. In the next section, two IPM design procedures are discussed in detail with the comparison of different optimization methods.

II. DESIGN PRACTICE

The interior permanent magnet machine is of special interest when the machine is required to be operated in extended speed range, due to the field weakening capability provided by the rotor side design. Moreover, the machine torque is partially provided by the reluctance torque from its salient construction due to the special configuration of embedded permanent magnets in the rotor iron. However, the necessary saturation regions in the rotor side make it difficult to create an accurate analytical model for the field distribution in the machine domain, which results in a difficult task for the machine performance evaluation in the whole speed range. FEA validation is a required phase for this type of machine design.

A modular machine structure design splits the conventional machine stator structure into segments and makes it possible to automate the winding mounting process, a labor intensive phase in the machine fabrication. With a modular structure, machine windings can be designed conveniently in a concentrically wound manner. The concentric winding reduces the loss and cost associated with the end winding sections compared to the conventional lap windings. Moreover, with proper selection of the module/pole number, the machine winding factor can be designed with a relatively high value, pushing up the machine power density. These benefits are associated with the modular machine structure and concentric winding design, so that applications of modular machine structures are gaining in popularity nowadays. With successive improvements of the power alloy technology, the soft magnetic composite (SMC) offers another option for the construction of machine modules simply by a single casting of iron powder with insulation mixture, which further simplifies the stator fabrication compared with the conventional lamination. In this paper, two IPM motor design optimizations with modular and conventional stator structure respectively are discussed.

A) Modular Stator Design

A preliminary modular machine structure (machine A) with a typical three phase four pole design is applied in the optimization practice as illustrated in Figure 2.

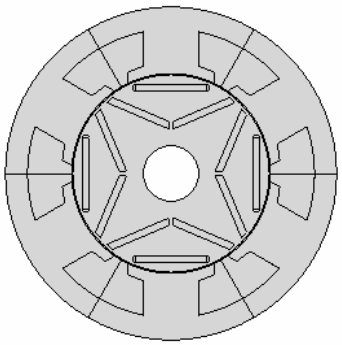

Figure 2: Machine A with modular stator

The machine stator side is assembled from six independent modules as the cross section of each module indicates in Figure 3 (a). From the design perspective, the machine performance is mainly determined by its geometric parameters with full knowledge of material properties. With dozens of design parameters, which is common for the definition of a specific machine structure, the design optimization turns into a time consuming process for virtually all methods. For instance, with only two FEA simulations at the upper and lower boundary points of design parameter space, it will cost 2^n simulations with a full but coarse experiment of design (EOD) information resulting. A simple comparison for the computational cost with regard to the parameter dimension is provided in Table 1 for this basic search, with 30 seconds for each FEA simulation assumed. The computation time can be scaled with different hardware bases, since the FEA consumes most of the CPU time.

Table 1: Computational cost with parameter dimension

n	10	15	20
Hours	8.53	273.1	8738.1

With an increased dimension, the computational cost makes it unrealistic to achieve a practical optimization problem if the solution space is fully searched at all boundaries, although various optimization strategies can mitigate this cost more or less. With a properly defined problem, the optimization process exhibits more effective solutions. Thus, the extraction of machine design parameter space turns out to be a crucial step for a successful optimization phase.

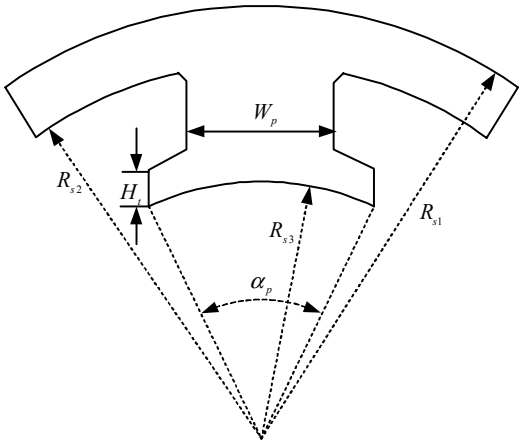

(a)

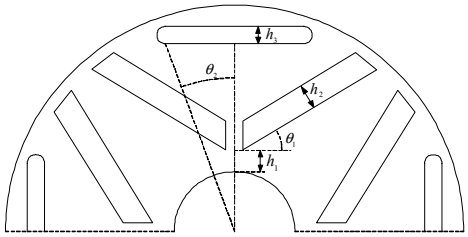

(b)

Figure 3: (a) Stator parameters. (b) Rotor parameters.

As illustrated in Figure 3, the stator module and rotor side geometries are basically defined by six and five main parameters respectively. Most of the other detailed geometric parameters can be obtained from these main parameters or are set with fabrication requirements, for example, the bridge width for the rotor cavity is fixed for a mechanical fabrication consideration. It should be mentioned that the air gap length is always a sensitive parameter, especially for small air gap machines. A slight adjustment of air gap length may result in a significant variation of machine performance, which makes it difficult to distinguish the impact of other design parameters. The loss of the tracking information obtained from previous simulations results in additional computation cost. Thus, in this example, the machine air gap is pre-selected.

The machine design results are compared by two optimization strategies based on Monte Carlo (MC) method and Deferential Evolution (DE) as provided in Table 2 and Table 3 with different optimization objectives.

Table 2: Optimized design for maximum torque T_{max}

Variables	MC	DE
R_{s2}	50.8mm	52.0mm
R_{s3}	34.5mm	36.1mm
W_p	21.0mm	20.2mm
H_t	4.2mm	4.5mm
α_p	45.9°	48.2°
h_1	2.2mm	2.48mm
h_2	3.5mm	4.7mm
h_3	4.9mm	4.6mm
θ_1	36.9°	39.1°
θ_2	20.1°	20.9°
T_{max}	6.32 Nm	6.85 Nm

In order to realize a design having a clean interface with the power supply, the THD of the back EMF is set as an optimization objective as well. With less harmonic components in machine's back EMF, the electromagnetic noise is reduced which also reduces machine torque pulsation and benefits sensorless control. The results are provided in Table 3.

Table 3: Optimized design for minimum back THD_{EMF}

Variables	MC	DE
R_{s2}	53.2mm	51.3mm
R_{s3}	33.5mm	35.2mm
W_p	18.0mm	22.7mm
H_t	4.7mm	5.1mm
α_p	43.6°	51.4°
h_1	6.2mm	7.0mm
h_2	2.5mm	2.8mm
h_3	2.4mm	2.5mm
θ_1	39.5°	40.2°
θ_2	20.1°	18.2°
THD_{EMF}	7.54%	8.48%

However, with the lower harmonics taken as an objective,

the machine torque for the solutions in Table 3 is affected as a result of the reduced flux. For instance, the torque optimized by DE is 4.60 Nm. In Table 4, optimized solutions with corresponding machine parameters are provided in the case of equally weighted objective functions of maximum torque and minimum harmonics.

Table 4: Optimal designs with multiple objectives

Variables	MC	DE
R_{s2}	53.2mm	52.1mm
R_{s3}	34.0mm	35.9mm
W_p	20.9mm	20.9mm
H_t	5.4mm	4.6mm
α_p	46.9°	50.5°
h_1	6.0 mm	6.1 mm
h_2	3.8 mm	3.2 mm
h_3	3.8 mm	3.7 mm
θ_1	34.2°	23.7°
θ_2	18.1°	27.2°
Torque	5.25 Nm	5.48 Nm
THD_{EMF}	16.5%	12.53%
L_d	18.9 mH	21.6 mH
L_q	24.9 mH	25.9 mH
Pout	989.6 W	1033 W
Efficiency (η)	89.6%	90.8%

The optimized machine structure and back EMF are illustrated in Figure 4.

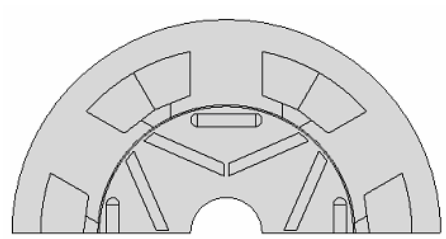

(a)

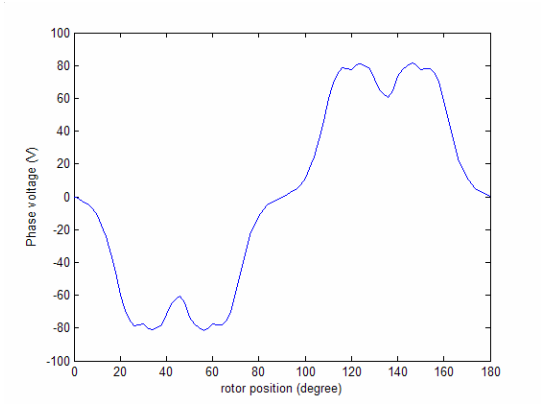

(b)

Figure 4: (a) Optimized geometry, (b) back EMF waveform

Due to the four pole, six slot design selection, the intrinsic cogging torque is evident with significant magnetic permeance variations along the air gap. With different rotor positions, the flux distribution pattern on the stator and rotor sides are different, which means that the winding flux linkages do not vary as ideal sinusoidal waveforms, resulting in the back EMF with high harmonic content. However with a high number slot design and better air gap flux distribution, the harmonic components can be reduced significantly.

B) Conventional Stator Design

A conventional stator IPM machine design (machine B) is also provided [5]. The machine is optimized for maximum electromagnetic torque at corner speed and maximum normalized characteristic current for the field weakening operation, with the constraints set as:

1. Minimum efficiency: η>0.85
2. Minimum torque: T>15Nm
3. Maximum flux density in stator core tooth: B_{ts}<1.8 T
4. Maximum flux density in the stator yoke: B_{ys}<1.5 T
5. Maximum rms linear current density: K_{1s}<22000 A/m
6. Maximum fundamental line-to-line back emf at maximum speed (6000 rpm) : 230 V rms

The main design variables are provided below in Table 5. Figure 5 provides the machine geometry with conventional stator and the design parameters.

Table 5: Design variables for machine B

	Variable	Variable type	Limits
1.	Ratio of stator inner diameter to outer diameter	continuous	$0.45 < D_s/D_o < 0.75$ ($D_o = 170$ mm)
2.	Ratio of stack length to maximum stack length	continuous	$0.6 < l_a/l_{a0} < 1$ ($l_{a0} = 150$ mm)
3.	Ratio of yoke thickness to difference between stator outer and inner radius	continuous	$0.2 < 2d_{ys}/(D_o - D_s) < 0.6$
4.	Permanent magnet data	discrete	Table input
5.	Number of pole pairs	integer	$p = 2, 3, 4, 5, 6$
6.	Ratio of tooth width to slot pitch at D_S	continuous	$0.3 < b_{ts}/\tau_s < 0.7$
7.	Ratio of total cavity to total rotor depth	continuous	$0.1 < \lambda_m < 0.5$
8.	Percentage of total cavity depth for inner cavity	continuous	$0.25 < \lambda_{h2} < 0.7$
9.	Percentage of total rotor depth for the outermost rotor core section	continuous	$0.2 < \lambda_{md1} < 0.6$
10.	Percentage of total rotor depth for middle rotor core section	continuous	$0.1 < \lambda_{md2} < 0.4$
11.	Angular span of the inner cavity relative to the pole pitch	continuous	$0.6 < \lambda_p < 0.95$
12.	The angle of the slanted magnet	continuous	$0.5 < \beta/\beta_0 < 1$, $\beta_0 = (1 - 1/p)\pi/2$

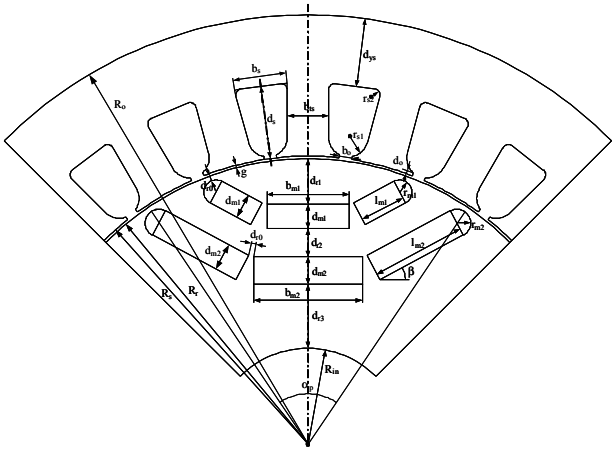

Figure 5: Machine B geometry,

Due to its complicated stator/rotor structure, machine B can

not be defined as simply as machine A. Some machine parameters which describe minor structural parameters of the geometry can be predefined and selected according to normal design practice, for example, rotor inner diameter. The constants of machine B are provided in Table 6.

Table 6: Constants for Machine B

Slot number	36
Poles	6
Stator outer diameter Do	170mm
Rotor inner diameter Di	38mm
Stack length	120mm
Air gap length	0.5mm
Stator tooth width	5.4mm
Stator yoke thickness	11.3mm
Slot opening width	2.5mm
Slot opening depth	0.6mm
Rotor bridge thickness	1.0mm
Slot corner radius	1.2mm
Armature current density	5.5 A/mm^2
Slot fill factor	0.4

With an acceptable time for the computation cost, the DE optimization process converges to a satisfactory design as plotted in Figure 5.

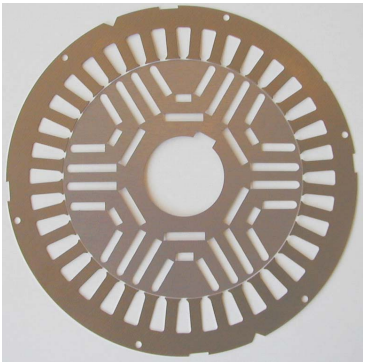

Figure 5: Laminations of the optimized IPM machine B

III. Optimization Vector Generation

The decisions that need to be made prior to the DE optimization are the size of the population and the values of the DE control parameter F and CR. The size of the population is usually dependent on the dimension of design parameter vector. In most cases, a good initial guess is to set the population size at 3-5 times larger than the number of design variables. If the population size is too small, there will not be enough variety among the members of the population. This can lead to a premature convergence to some local minimum. Alternatively, if the population size is too large, then a much greater computational time will be required to evaluate all the members of the population without significantly reducing the number of generations needed to reach the optimal solution. The values of the DE control parameters F and CR which would lead to the fast convergence cannot be determined in a straightforward manner. Therefore, several preliminary executions of DE algorithm have been carried out for different combination of F and CR to observe their influence on the final results and determine which combination is the best for each particular motor design optimization. These parameters also affect the total number of non-dominant solutions in the Pareto set that can be found in a given number of iterations which is another important issue in multi-objective optimization.

The values of the objective functions for the solutions in the Pareto set calculated using different combinations of DE control parameters F and CR have been plotted in Figure 6.

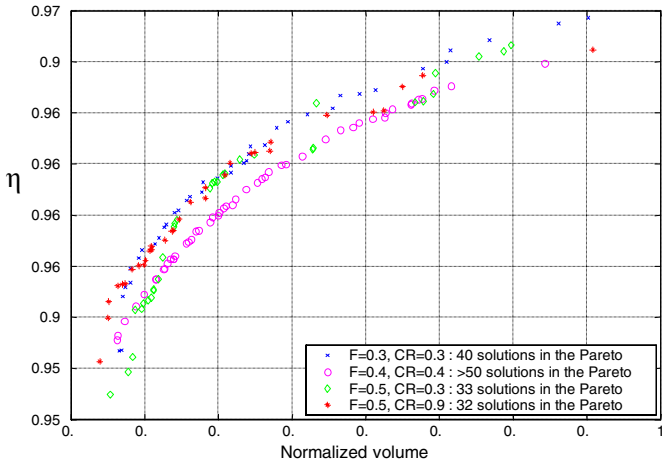

Figure 6: Pareto fronts resulting from F,CR combinations

It appears that for the designs considered, F=0.3 and CR=0.3 is the best choice among possible combinations because it yields the highest efficiency for any volume of the motor. The slope of the Pareto front reduces as both the efficiency and active volume increases. This means that initially at lower values of efficiency an increase in volume yields a higher increase in efficiency. The choice of the solution in the Pareto set must be determined by the designer, based on the priority where higher importance can be given to a smaller size motor while sacrificing the efficiency or vice versa. Other compromises can be selected recognizing that a choice exists among an entire set of solutions. This procedure provides insight into the design trade-offs and is the main benefit of the multi-objective optimization.

IV. Experimental Results

Two prototype motors based on the designs previously discussed have been fabricated and tested as illustrated in Figure 7. For machine A, a fully extended testing is under way and the results will be reported soon in a future paper. Figure 8 illustrates the roughly measured back EMF of machine A. Significant noise can be observed in Figure 8 due to the machine vibrations during testing, while the averaged back

EMF waveform is fairly matched with the prediction by the optimization results.

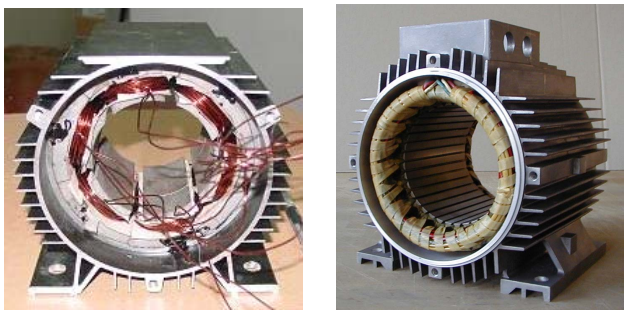

Machine A Machine B

Figure 7: Prototypes

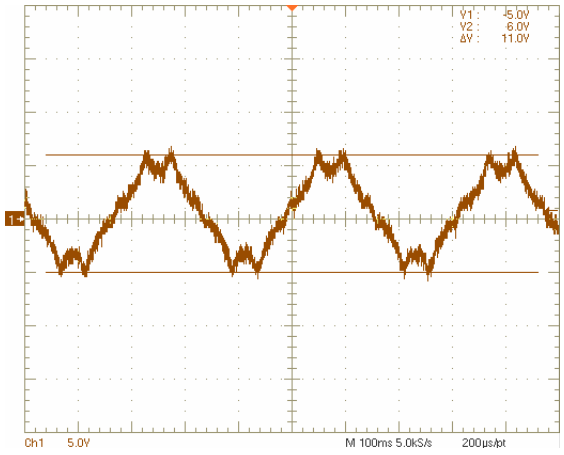

Figure 8: Back EMF for machine A

For machine B, the testing has been fully carried out. The L_d and L_q are measured and compared with the optimized results as provided in Figure 9 and Figure 10.

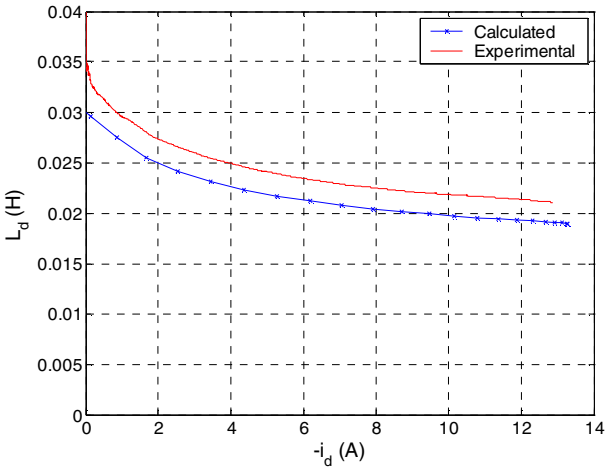

Figure 9: Inductance measurement L_d for machine B

For motor mode operation, i_d is negative and i_q is positive, which means the inductance plot L_d vs i_d for $i_d < 0$ and L_q vs. i_q for $i_q > 0$ are usually of interest. In Figure 9, the measured machine d axis inductance is slightly higher than calculated value, while the L_q is about 20% lower than the design prediction in the lower and higher end of the I_q range, which may be attributed to the tolerances in laminations cuts or altered magnetic properties of the lamination material in the fabrication phase.

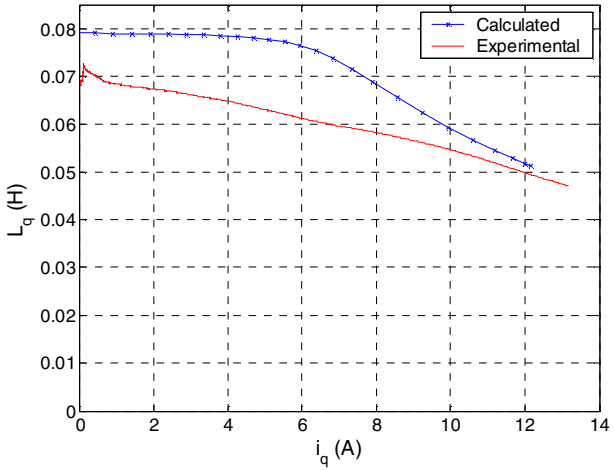

Figure 10: Inductance measurement L_q for machine B

Due to the loss of L_q, the torque and extended speed operation deviate from the design curve as illustrated in Figure 11.

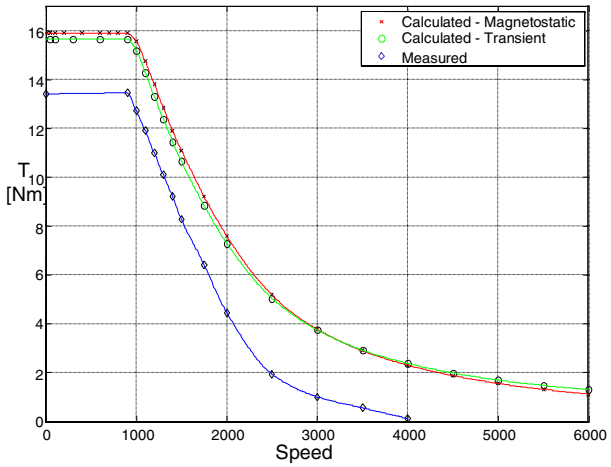

Figure 11: Torque vs. Speed for machine B

V. CONCLUSION

In this paper, the Differential Evolution (DE) has been introduced as a reliable method for the design optimization which can solve single and multi-objective optimization problems. The effectiveness of the method has been shown on examples of optimized design of two interior PM motor designs with modular stator and conventional stator respectively. The

effectiveness of this design method is validated by the final test results.

REFERENCES

[1] E.C. Lovelace, T.M. Jahns and J.H. Lang, "Impact of saturation and inverter cost on interior PM synchronous machine drive optimization", Industry Applications, IEEE Transactions on Volume 36, Issue 3, May-June 2000 Page(s):723 – 729

[2] Ch. Schatzer, A. Binder.; "Design optimization of a high-speed permanent magnet machine with the VEKOPT algorithm**",** Industry Applications Conference, 2000. Conference Record of the 2000 IEEE, Volume 1, 8-12 Oct. 2000 Page(s):439 - 444 vol.1

[3] J. Wang; D. Howe, "Tubular modular permanent-magnet machines equipped with quasi-Halbach magnetized magnets-part II: armature reaction and design optimization", Magnetics, IEEE Transactions on Volume 41, Issue 9, Sept. 2005 Page(s):2479 – 2489

[4] R. Storn and K. Price, "Differential Evolution – a Simple and Efficient Adaptive Scheme for Global Optimization over Continuous Spaces", Technical Report TR-95-012, ICSI, March, 1995.

[5] Damir Zarko, "*A systematic approach to optimized design of permanent magnet motors with reduced torque pulsations*". Ph.D thesis, University of Wisconsin – Madison, 2004.